Computational Screening of the Physical Properties of Water-in-Salt Electrolytes

Trinidad Mendez-morales, Trinidad Méndez-Morales, Zhujie Li, Mathieu Salanne

Computational Screening of the Physical Properties of Water-in-Salt Electrolytes

Trinidad Mendez-Morales,[†,‡,¶] Zhujie Li,[†,‡,¶] and Mathieu Salanne[*,†,‡,¶,§]

†*Maison de la Simulation CEA, CNRS, Université Paris-Sud, UVSQ, Université Paris-Saclay, F-91191 Gif-sur-Yvette, France*

‡*Sorbonne Université, CNRS, Physico-Chimie des Électrolytes et Nanosystèmes Interfaciaux, F-75005 Paris, France*

¶*Réseau sur le Stockage Électrochimique de l'Énergie (RS2E), FR CNRS 3459, Amiens, France*

§*Institut Universitaire de France (IUF), 75231 Paris Cedex 05, France*

E-mail: mathieu.salanne@sorbonne-universite.fr

Abstract

Water-in-salts form a new family of electrolytes with properties distinct from the ones of conventional aqueous systems and ionic liquids. They are currently investigated for Li-ion batteries and supercapacitors applications, but to date most of the focus was put on the system based on the LiTFSI salt. Here we study the structure and the dynamics of a series of water-in-salts with different anions. They have a similar parent structure but they vary systematically through their symmetric/asymmetric feature and the length of the fluorocarbonated chains. The simulations allow to determine their tendency to nanosegregate, as well as their transport properties (viscosity, ionic conductivity, diffusion coefficients) and the amount of free water, providing useful data for potential applications in energy storage devices.

1 Introduction

Lithium-ion batteries (LIBs) involve organic electrolytes, which allows them to reach high voltages and thus increases the energy density of the devices.[1] However, some concerns remain associated with their cost, safety and environmental impact.[2,3] Aqueous electrolytes can be an alternative to solve these problems, but the use of water as solvent results in a much narrower electrochemical stability window.[4,5] Recently, a new class of water-in-salt (WiS) electrolytes was reported by Suo *et al.*[6] to expand the electrochemical stability window up to nearly 3 V by using aqueous solutions of lithium bis[(trifluoromethyl)sulfonyl]imide (LiTFSI) with a molality of 21 m (mol/kg). In such superconcentrated electrolytes the increased stability window is due to several effects:[7] Firstly, water molecules display a specific speciation, since most of them belong to the lithium ion solvation shells, thus leading to low fractions of free water molecules. This reduces the concentration of water at the positive interface, which mainly contains $TFSI^-$ anions.[6,8] However, the main reason for the extended voltage window is the formation of a solid electrolyte interface (SEI) layer that mainly consists of LiF as a result of the electrochemical decomposition of the TFSI anion.[9–11] Although most of the studies of WiS electrolytes were performed using the LiTFSI salt,[12–16] the WiS concept was extended to other metallic ions such as potassium,[17] sodium[18–20] and zinc-based[21] electrolytes.[22]

In parallel, the chemistry of Li-ion based WiS electrolyte family was also explored further. For example, since the concentration of LiTFSI in the WiS electrolyte is limited by the solubility limit, it was proposed to mix them with other salts to increase further the electrochemical stability window.[23–25] On the contrary, the WiS electrolytes form biphasic systems when they are mixed with simpler solutions such as highly concentrated aqueous LiCl,[26] which was exploited to develop a dual battery involving lithium ions together with halogen conversion-intercalation.[27] Greener and lower-cost alternatives to fluorinated compounds would also be preferable; in order to fulfil this objective WiS based on the acetate anion instead of TFSI were also proposed,[28–30] showing further the versatility of this family of

electrolytes. Other solvents, such as glymes, are also widely investigated for the development of superconcentrated electrolytes.[31,32]

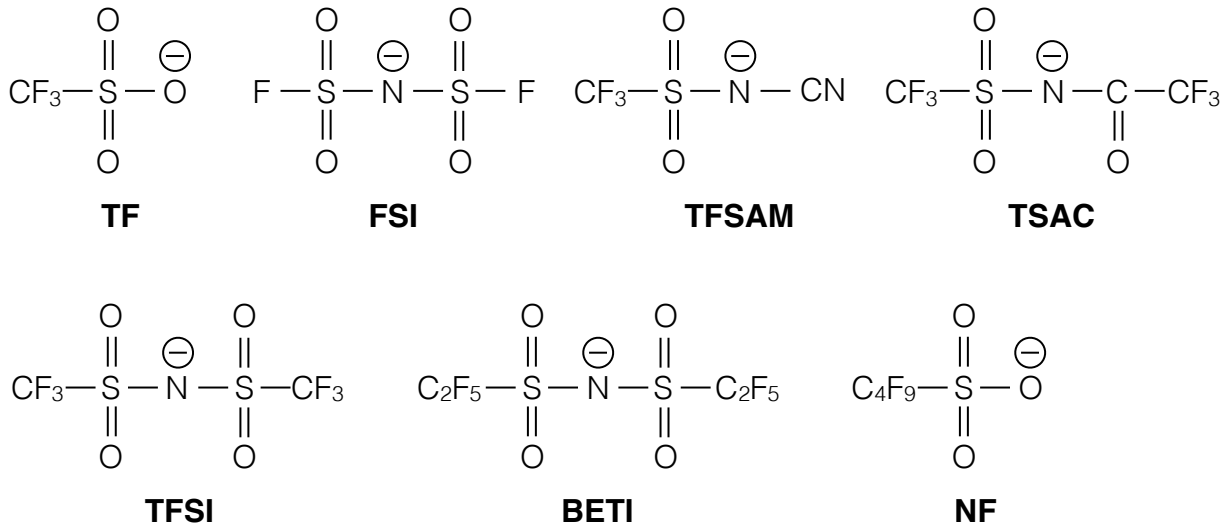

Figure 1: Chemical formulae of the various anions investigated in this work. The full names of the molecules are trifluoromethanesulfonate (TF), bis(fluorosulfonyl)imide (FSI), 2,2,2-trifluoromethylsulfonyl-N-cyanoamide (TFSAM), 2,2,2-trifluoro-N-(trifluoromethylsulfonyl) acetamide (TSAC), bis[(trifluoromethyl)sulfonyl]imide (TFSI), bis[(pentafluoroethyl)sulfonyl]imide (BETI) and nonafluorobutanesulfonate (NF).

In practice, it could be possible to develop WiS electrolytes with a large number of different anions. Here we show that molecular dynamics (MD) simulations provide a convenient framework for studying their physical properties. We studied seven different anions, including five which were imide-based, namely bis[(trifluoromethyl)sulfonyl]imide (TFSI), bis(fluorosulfonyl)imide (FSI), bis[(pentafluoroethyl)sulfonyl]imide (BETI), 2,2,2-trifluoromethylsulfonyl-N-cyanoamide (TFSAM) and 2,2,2-trifluoro-N-(trifluoromethylsulfonyl) acetamide (TSAC), and two sulfonate anions, trifluoromethanesulfonate (TF) and nonafluorobutanesulfonate (NF). Their chemical formulae are provided on Figure 1. The same force field is used for all the ions[33] in order to ensure systematic comparisons of their properties. We first study the structure at a large molality of 15 mol kg^{-1} so that the salt/water ratio is similar for all the systems. We then compare the conductivity, the viscosity of the liquids as well as the individual diffusion coefficients of all the species. Comparing these transport properties

allows to rank the various anionic species for applications. Finally, we determine the amount of "free" water in the various systems since this quantity is known to influence the reactivity at the electrochemical interface.

2 Results and Discussion

Among all the mixtures considered in this article, the only one for which there is available experimental data concerning the solubility limit is LiTFSI-H_2O, whose value was reported to be a molality of 31.3 m at 303.15 K.[15] Accurately computing solubilities is very challenging in molecular dynamics,[34] so that we decided to analyze the medium/long range structure as a proxy to determine the relative miscibility of the systems. To do this, partial structure factors were computed using the formalism proposed by Faber and Ziman,[35] in which the structure factor is represented by the correlations between the different chemical species α and β:

$$S_{\alpha\beta}(q) = 1 + 4\pi\rho \int_0^\infty dr \frac{\sin(qr)}{qr} r^2 (g_{\alpha\beta}(r) - 1) \tag{1}$$

where $g_{\alpha\beta}(r)$ are the partial radial distribution functions (RDFs) and ρ is the number density of the system (all the RDFs are provided as Supplementary Data).

Figure 2 shows the partial structure factors of (a) S-S and (b) O(H_2O)-O(H_2O) atoms in the different mixtures. The LiNF-based system shows very distinct features, as indicated by the peak at $q \to 0$. This points towards the formation of long-ranged structural features. This is confirmed by the snapshots of the simulation box included in Figure 2, in which we can clearly observe the formation of nanodomains consisting in the apolar (composed of the CF_2- and CF_3-groups of the NF-anion, see panel (c)) and polar (consisting of lithium atoms, water molecules and the negatively charged SO_3-group of the NF-anion, see panel (d)) components of the liquid. This feature is reminiscent to the formation of supramolecular arrangements similar to the ones which form in mixtures of ethylammonium nitrate ionic

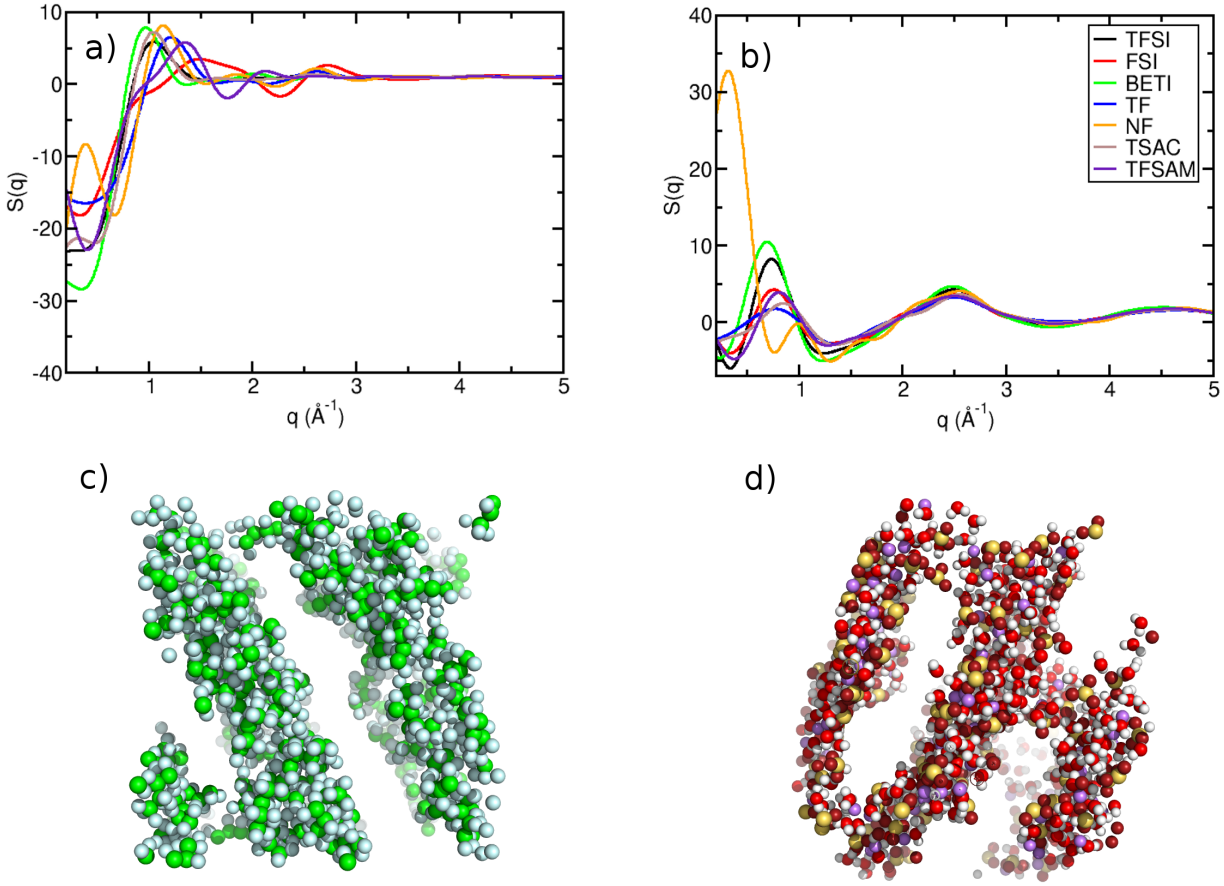

Figure 2: Partial structure factors of (a) S-S and (b) O(H_2O)-O(H_2O) atoms from MD simulations at 298.15 K for all the different mixtures. Snapshots of the simulation box that shows long-ranged ordering of the LiNF-H_2O system into (c) apolar (composed of C and F atoms, in green and light blue, respectively) and (d) polar (consisting of lithium atoms in violet, H_2O molecules in white and light red, and S and O atoms, in yellow and dark red, respectively) domains.

liquid with nonamphiphilic compounds[36,37] or of ionic liquids with acetonitrile,[38] but it may point a low LiNF solubility in water that should be confirmed experimentally. All the other simulated WiS show similar structures, *i.e.* the formation of medium-ranged nano-heterogeneities[12] at medium range as can be seen from the presence of intense peaks at q values ranging from 0.95 to 1.5 Å^{-1} and from 0.7 to 0.9 Å^{-1} for the S-S and the O-O partial structure factors, respectively.

The use of WiS as electrolytes in energy storage devices will then be a compromise between a high concentration to extend the electrochemical stability window and a good

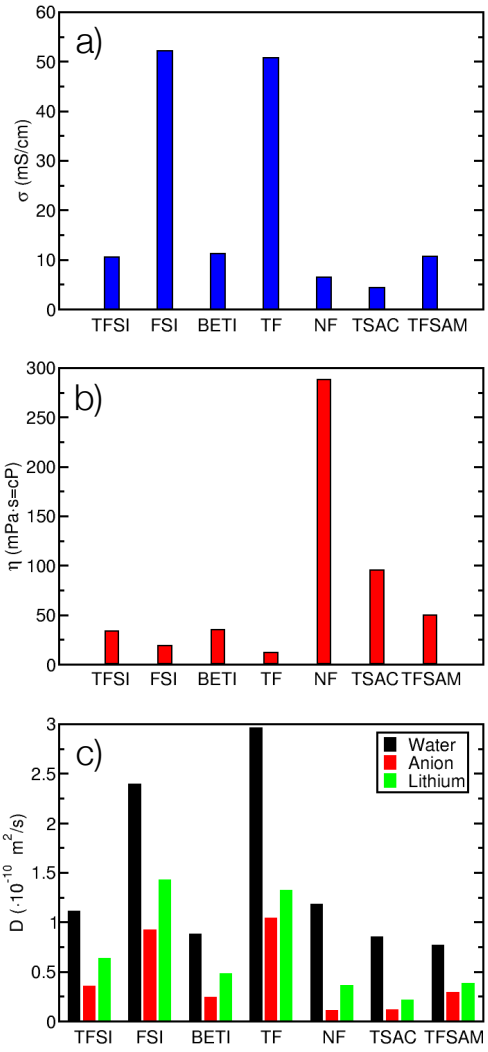

Figure 3: Comparison of the transport properties of the WiS electrolytes at room temperature. (a) ionic conductivity; (b) viscosity; (c) diffusion coefficients.

ionic conductivity that guarantees acceptable power density.[15,16,39] Thus, the tailored design of superconcentrated aqueous electrolyte systems requires a deep understanding of the ion transport mechanism,[40] and several reports suggested a fast Li ion transport through water-rich domains.[12,13] The two key collective transport quantities are the electrical conductivity and the viscosity. The former can be calculated in molecular dynamics simulations using

$$\sigma = \frac{e^2}{k_B T V} \lim_{t\to\infty} \frac{1}{6t} \langle | \sum_i q_i \Delta_i(t) |^2 \rangle \tag{2}$$

where e is the elementary charge, V is the volume of the simulation cell, T is the temperature,

k_B is the Boltzmann constant and $\Delta_i(t) = \vec{r}_i(t) - \vec{r}_i(0)$ is the displacement of the ion i, which carries a charge q_i, over a time interval t (brackets $\langle ... \rangle$ indicate an ensemble average). This expression includes the contribution not only of the self-terms of each ion but also the complex effect of cross-correlations due to the correlated motion of ions. The electrical conductivities obtained using Eq.(2) are included in Figure 3a.

The shear viscosity of the electrolytes was computed within the Green-Kubo (GK) formalism[41] by integration of the stress-tensor correlation function

$$\eta = \frac{V}{k_B T} \int_0^\infty \langle \Pi_{\alpha\beta}(0) \Pi_{\alpha\beta}(t) \rangle dt \tag{3}$$

where $\Pi_{\alpha\beta}$ represents any of the five independent components of the stress tensor, Π_{xy}, Π_{xz}, Π_{yz}, Π_{xx-yy}, $\Pi_{2zz-xx-yy}$. The values obtained for the viscosity of each system, that is, the value of the plateau at which the running integral in Eq.(3) converges after a certain time, are shown in Figure 3b.

The simulations predict a LiTFSI-H_2O viscosity in good agreement with experimental data ($\approx$ 33 cP instead of 22 cP[42]), while they underestimate the ionic conductivity by a factor 2,[6,15,42] which corresponds to typical error for the prediction of transport properties in electrolytes by non-polarizable molecular dynamics.[43] Although the use of a different parameterization for the partial charges and Lennard-Jones parameters of the anion could improve the situation,[42] the present parameters were chosen in order to keep consistency between all the different anions studied and to compare them without introducing any bias.

When comparing the various liquids, we observe that they can be separated between three groups. Firstly, the superconcentrated LiFSI-H_2O and LiTF-H_2O mixtures have low viscosities and high ionic conductivities. In particular, the latter ($\sim$ 50 mS/cm in both cases) is greater than the values observed in typical non-aqueous electrolytes used in commercial Li-ion batteries[44] and supercapacitors.[45] Then we observe that the LiBETI-H_2O mixture shows similar performances as the reference TFSI system. The LiTFSAM-H_2O has a larger viscosity but a simular conductivity as those two, so it can be put in the same group. Finally,

the systems involving the TSAC and NF anions show significantly poorer performances than all the others, with viscosities reaching $\sim$ 100 cP and 300 cP, respectively, and a low ionic conductivity. It is worth noting that the variations between anions cannot easily be explained using their relative size/weights since for example TFSAM and FSI have relatively similar sizes, as well as TFSI and TSAC, while BETI has the largest fluorocarbonated chains. Nevertheless, if we split them between the symmetric (FSI, TFSI and BETI by order of increasing size) and asymmetric (TF, TFSAM, TSAC and NF) ones, we observe a trend for the viscosity to increase with the anion size. Based on this observation, the best transport properties seem to arise for small symmetric anions.

In order to analyze further the individual dynamics of the liquids, the self-diffusion coefficient of the species i can be calculated from the long-time limit of the mean-squared displacement (MSD) using

$$D_i = \lim_{t\to\infty} \frac{1}{6t} \langle |\Delta_i(t)|^2 \rangle \tag{4}$$

Note that a correction due to the use of periodic boundary conditions must be added.[46] Figure 3c shows the values obtained for H_2O molecules, lithium cations and the various anions. In agreement with previous works,[12,42] it can be seen that water molecules are the most mobile species, followed by lithium cations and anions. This corresponds to an opposite behaviour with respect to the dynamics of the ions in typical ionic liquid electrolytes, where anions generally diffuse faster than cations.[12,39,47]

The individual dynamics provide further points of comparison between the various electrolytes. The main difference with respect to the analysis of the collective transport properties is that the diffusivity of water molecules in the TSAC and NF-based system are similar to the cases of TFSI, BETI and TFSAM. This points towards a predominant role of the low diffusivity of the anions in the high viscosity of the system. We also observe that the lithium ion dynamics is enhanced in LiTFSI-H_2O with respect to BETI and TFSAM-based systems, which points towards a better performance of the former in Li-ion batteries applications

despite the similar conductivities of the systems.

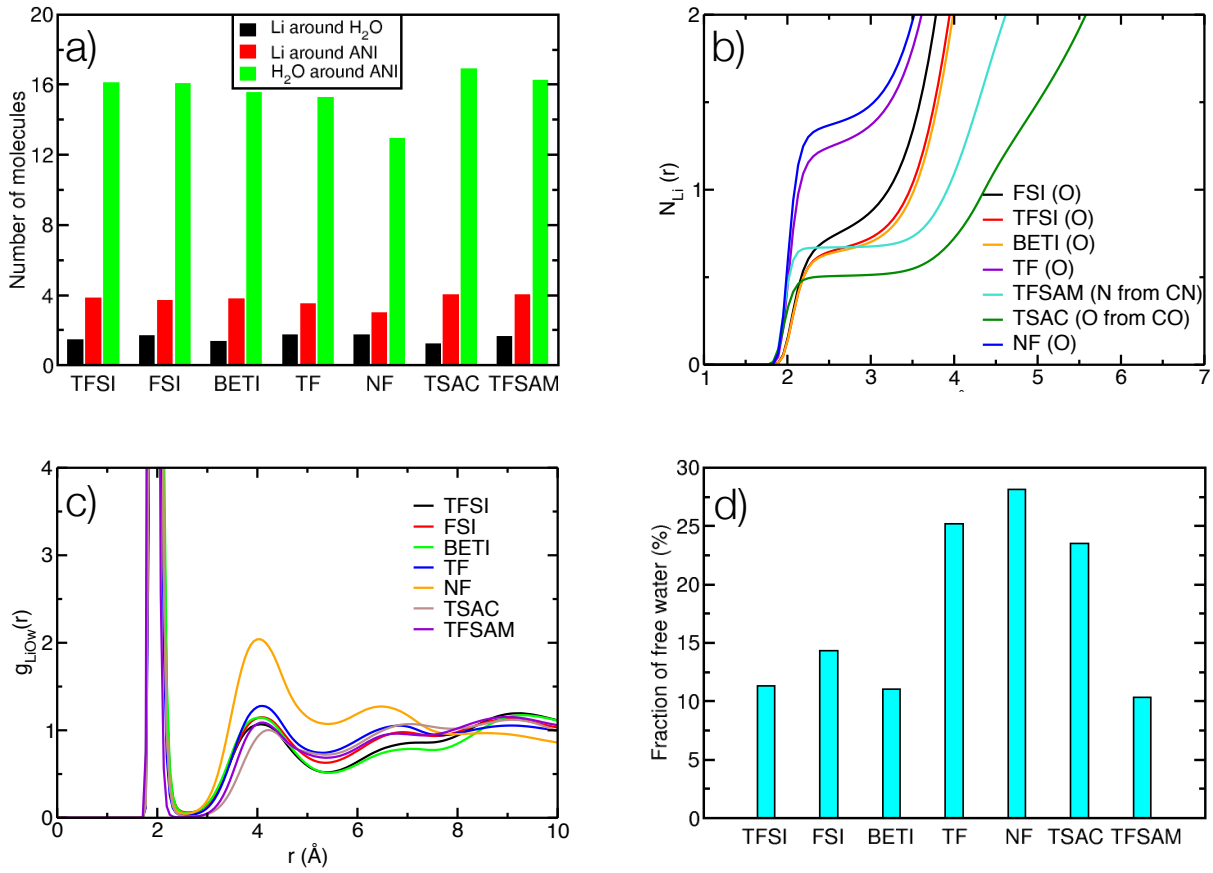

Figure 4: a) Neighbour count around the reference subset from Voronoi analysis for the different mixtures. b) Running coordination number around the lithium ions of their closest atom from each anion. c) Radial distribution function between the lithium ion and the oxygen from water molecules (Ow) for all the systems. d) Fraction of free water not bound to any Li cation obtained for the different mixtures.

Unlike in ionic liquid/water systems, where the interaction between H_2O molecules and anions is generally stronger than with the cations,[48] in the studied WiS electrolytes they are strongly attracted by the lithium ions[6] (note that this is due to the hydrophobicity of the fluorinated anions, different effects are expected in acetate-based water-in-salts[28–30]). This effect was recently used by Chen *et al.* to expand the voltage window of humid ionic liquids.[49] At infinite dilution the first solvation shell of Li^+ is made of four water molecules. At the molality studied here, the ratio H_2O/Li is smaller than four. As a consequence the first solvation shell of lithium cations includes both water and anions. It was previously

reported that as the concentration of the mixture increases the coordination environment is expected to change from solvent-separated ion pairs to a majority of contact ion pairs and even ionic aggregates.[12,18,50] In the present work, we employed the trajectory analysis program TRAVIS[51] to analyze the coordination of the molecules in these electrolytes. Its methodology is based on Voronoi tessellation:[52,53] The subsets were defined so as to match the three types of molecules (anions, water and lithium) in the mixtures, and two subsets were considered to be neighbours if they share at least a common face. This approach provided us with valuable information on the neighborhood of the reference subset, and the results are included in Figure 4a. We can observe that the choice of the anion does not have a remarkable impact on the number of molecules neighbouring a reference one, so that the WiS studied here have qualitatively similar structures. The main difference concerns the NF-based system, for which the number of H_2O molecules around each anion is smaller than in the other systems, reflecting the highest hydrophobicity of this anion. This is at the origin of the supramolecular organization described above. We have therefore analyzed further the local structure by computing all the partial RDFs of the system (these are provided as Supplementary Data, and the partial functions involving the lithium ions and the atoms from the various anions are displayed on Supplementary Figures S2 and S3). Again, we do not observe large difference in the cation-anion structure: In all cases, the interaction occurs preferentially via one site, generally the oxygen from the S=O groups (except for TFSAM, for which it is the N atom from the C≡N group and TSAC, for which it is the O from the C=O group). The intensity of the corresponding peak in the RDF vary from one system to another, which mostly reflects the number of the corresponding sites within each ion. In order to deconvolute this effect, we have computed the running coordination number around the lithium ions:

$$N^i_{\mathrm{Li}}(r) = \rho_i \int_0^r g_{\mathrm{Li}-i}(r')4\pi r' \mathrm{d}r' \tag{5}$$

where ρ_i is the number density of atom type i. These functions are shown on Figure 4b.

Firstly, we observe that the TF and the NF have larger coordination numbers than the other anions, but it is worth noting that in these species the three oxygen atoms bounded to the sulphur are adjacent, so the existence of bidentate coordination for the lithium atoms is probably at the origin of this behaviour. We then compare the three symmetric anions and the two asymmetric ones. FSI, TFSI and BETI show very similar coordination numbers, which again is coherent with the fact that the corresponding systems have comparable properties. Then the TFSAM and TSAC display smaller coordination numbers, but the shape of the $N^i_{\mathrm{Li}}(r)$, with a long plateau after the first solvation shell, indicates that the corresponding bonds are stronger than in the other systems. In these asymmetric systems, the charge is not evenly distributed which explains why the lithium have preferential interactions with the highly-charged moiety. Such ionic bonds pin the aqueous network to the anionic nanodomains, which may provide an interpretation for the larger viscosities of the corresponding water-in-salts.

The small variations observed for the coordination of the Li ions by the water molecules (Figure 4a) may lead to substantial changes in the concentration of "free" water molecules at such molalities. The partial RDFs between the lithium and the oxygen atoms from the water molecules are shown on Figure 4c. A water molecule is considered to be free when it is not coordinated to any lithium ion, *i.e.* when the corresponding shortest distance is larger than the first minimum of the RDF (but it is worth noting that in WiS they remain partly coordinated to other water molecules through an extended hydrogen-bond network, which will affect their reactivity as well[54]). The amount of free water molecules is shown in Figure 4b. We observe that it is significantly higher in the TF, TSAC and NF-based systems. This probably affects significantly the electrochemical window because non-coordinated water molecules can adsorb more easily on the positive electrode than the lithium-coordinated ones (due to the Coulombic repulsion of the Li^+ ions). At the negative electrode it is also expected that the formation of the protective SEI will be more difficult for these salts. Nevertheless, simulation of electrode/electrolyte interfaces would be necessary

to confirm this point.[54]

3 Conclusions

In conclusion, we have studied through extended molecular dynamics simulations a series of WiS electrolytes where the nature of the anion was systematically changed. The same force field was used for all the simulations and the molality was kept fixed at 15 m in order to allow for representative comparisons. By analyzing the structure factors, we observed that the NF-based system has a strong tendency to form large-scale domains in which the polar groups and water molecules are strongly segregated from the highly hydrophobic fluorinated chains of the NF anions. All the other anions have structural features typical of water-in-salts, namely the formation of nanoheterogeneities with two type of domains, the first ones containing mostly the anions and the second ones made of solvated lithium ions linked through the hydrogen-bond network of the water molecules.

In a second step, by computing the transport properties we have identified that they do not vary in a systematic way with the size or the molecular weight of the anion. For a given ion size, the use of symmetric anions leads to a lower viscosity and increased ionic conductivities and diffusion coefficients. The TF and FSI display higher diffusion coefficients, followed by the TFSI, BETI and TFSAM-based systems. Finally, the TSAC and NF have poor viscosities and should therefore be avoided in electrochemical systems.

Finally, we have looked at the speciation of the systems, we have observed that the TF-based system has a relatively high amount of free water molecules, which may affect its electrochemical window. Nevertheless, future work should adress more specifically the reactivity of the molecules since the mechanisms that have been identified for TFSI may not be adequate for all the other anions. This will require the use of density functional theory-based simulations in order to allow the formation/break of chemical bonds.

Simulation details

MD simulations of WiS electrolytes were carried out using the LAMMPS package[55] (typical input files for all the systems are provided as Supplementary Data). All cubic simulation boxes contained 473 water molecules and 128 salt ion pairs that were randomly distributed using Packmol.[56] The SPC/E water model was used in these simulations,[57] whereas the parameterization of the anions was made in the framework of the CL&P[58] force field for ionic liquids, for which we employed the set of parameters reported in Ref. 33. Lithium cations were modelled as a single site whose Lennard-Jones (LJ) parameters are $\epsilon = 6.25$ kcal/mol and $\sigma = 1.25992$ Å. It must be noted that the charges of both ions were uniformly scaled by a factor of 0.8 so as to accelerate the dynamics of the mixtures, which was shown necessary to have good agreement with the experimental results in LiTFSI WiS.[42]

Table 1: Densities obtained for the seven WiS electrolytes at a concentration of 15 m and room temperature. The experimental density of a water/LiTFSI mixture under the same conditions[42] is 1673 kg/m^3.

Lithium salt	**Density (kg/m^3)**
LiTFSI	1692.577
LiFSI	1631.462
LiBETI	1751.465
LiTF	1570.122
LiNF	1770.777
LiTFSAM	1533.237
LiTSAC	1680.515

In order to reach proper density, each system was firstly equilibrated at 298.15 K and 1 bar for 4 ns in the NpT ensemble by using Nosé-Hoover thermostat and barostat[59–61] with relaxation times of 10 and 500 femtoseconds, respectively. The results are included in Table 1; an error of 1 % w.r.t. experimental data is obtained for the LiTFSI-based liquid[42] (no data is available for the other systems). Then we performed a second equilibration of 60 ns within an NVT ensemble, followed by a production run of around 90 ns (with a time step $dt = 1$ fs) that was used to obtain structural and dynamic information about the systems.

Data accessibility statement

The data that support the findings of this study are openly available on the repository https://gitlab.com/ampere2/mendezmorales_2020 and on Zenodo (http://dx.doi.org/10.5281/zenodo.4293

Acknowledgments

This work was supported by the French National Research Agency (Labex STORE-EX, Grant No. ANR-10-LABX-0076, and ANR BALWISE, Grant No. ANR-19-CE05-0014). This project has received funding from the European Research Council (ERC) under the European Union's Horizon 2020 research and innovation programme (grant agreement no. 771294).We acknowledge support from EoCoE, a project funded by the European Union Contract No. H2020-EINFRA-2015-1-676629, from the DSM-Energie programme of CEA and from the Eurotalent programme. This work was granted access to the HPC resources of CINES under the allocation A0080910463 made by GENCI.

References

(1) Armand, M.; Tarascon, J. M. Building better batteries. *Nature* **2008**, *451*, 652–657.

(2) Grey, C. P.; Tarascon, J. M. Sustainability and in situ monitoring in battery development. *Nature* **2016**, *16*, 45–56.

(3) Hammami, A.; Raymond, N.; Armand, M. Lithium-ion batteries: runaway risk of forming toxic compounds. *Nature* **2003**, *424*, 635–636.

(4) Wang, Y.; Yi, J.; Xia, Y. Recent Progress in Aqueous Lithium-Ion Batteries. *Adv. Energy Mater.* **2012**, *2*, 830–840.

(5) Wessells, C.; Huggins, R. A.; Cui, Y. Recent results on aqueous electrolyte cells. *J. Power Sources* **2011**, *196*, 2884–2888.

(6) Suo, L.; Borodin, O.; Gao, T.; Olguin, M.; Ho, J.; Fan, X.; Luo, C.; Wang, C.; Xu, K. "Water-in-salt" electrolyte enables high-voltage aqueous lithium-ion chemistries. *Science* **2015**, *350*, 938–943.

(7) Borodin, O.; Self, J.; Persson, K. A.; Wang, C.; Xu, K. Uncharted Waters: Super-Concentrated Electrolytes. *Joule* **2020**, *4*, 69–100.

(8) Li, Z.; Jeanmairet, G.; Mendez-Morales, T.; Rotenberg, B.; Salanne, M. Capacitive performance of water-in-salt electrolytes in supercapacitors: a simulation study. *J. Phys. Chem. C* **2018**, *122*, 23917–23924.

(9) Dubouis, N.; Lemaire, P.; Mirvaux, B.; Salager, E.; Deschamps, M.; Grimaud, A. The role of the hydrogen evolution reaction in the solid–electrolyte interphase formation mechanism for "Water-in-Salt" electrolytes. *Energy Environ. Sci.* **2018**, *11*, 3491–3499.

(10) Bouchal, R.; Li, Z.; Bongu, C.; Le Vot, S.; Berthelot, R.; Rotenberg, B.; Favier, F.; Freunberger, S.; Salanne, M.; Fontaine, O. Competitive Salt Precipitation/Dissolution During Free-Water Reduction in Water-in-Salt Electrolyte. *Angew. Chem., Int. Ed.* **2020**, *59*, 15913–15917.

(11) Steinrück, H.-G.; Cao, C.; Lukatskaya, M.; Takacs, C.; Wan, G.; Mackanic, D.; Tsao, Y.; Zhao, J.; Helms, B.; Xu, K.; Borodin, O.; Wishart, J. F.; Toney, M. Interfacial Speciation Determines Interfacial Chemistry: X-ray-Induced Lithium Fluoride Formation from Water-in-salt Electrolytes on Solid Surfaces. *Angew. Chem., Int. Ed.* **2020**, *in press*, 10.1002/ange.202007745.

(12) Borodin, O. et al. Liquid Structure with Nano-Heterogeneity Promotes Cationic Transport in Concentrated Electrolytes. *ACS Nano* **2017**, *11*, 10462–10471.

(13) Lim, J.; Park, K.; Lee, H.; Kim, J.; Kwak, K.; Cho, M. Nanometric Water Channels in Water-in-Salt Lithium Ion Battery Electrolyte. *J. Am. Chem. Soc.* **2018**, *140*, 15661–15667.

(14) Coustan, L.; Shul, G.; Bélanger, D. Electrochemical behavior of platinum, gold and glassy carbon electrodes in water-in-salt electrolyte. *Electrochem. Commun.* **2017**, *77*, 89–92.

(15) Lannelongue, P.; Bouchal, R.; Mourad, E.; Bodin, C.; Olarte, M.; le Vot, S.; Favier, F.; Fontaine, O. "Water-in-Salt" for Supercapacitors: A Compromise between Voltage, Power Density, Energy Density and Stability. *J. Electrochem. Soc.* **2018**, *165*, A657–A663.

(16) Dou, Q.; Lei, S.; W., D.-W.; Zhang, Q.; Xiao, D.; Guo, H.; Wang, A.; Yang, H.; Li, Y.; Shi, S.; Yan, X. Safe and high-rate supercapacitors based on an "acetonitrile/water in salt" hybrid electrolyte. *Energy Environ. Sci.* **2018**, *11*, 3212–3219.

(17) Leonard, D. P.; Wei, Z.; Chen, G.; Du, F.; Ji, X. Water-in-Salt Electrolyte for Potassium-Ion Batteries. *ACS Energy Lett.* **2018**, *3*, 373–374.

(18) Suo, L.; Borodin, O.; Wang, Y.; Rong, X.; Sun, W.; Fan, X.; Xu, S.; Schroeder, M. A.; Cresce, A. V.; Wang, F.; Yang, C.; Hu, Y.; Xu, K.; Wang, C. "Water-in-Salt" Electrolyte Makes Aqueous Sodium-Ion Battery Safe, Green, and Long-Lasting. *Adv. Energy Mater.* **2017**, *7*, 1701189(1)–1701189(10).

(19) Kuhnel, R. S.; Reber, D.; Battaglia, C. A High-Voltage Aqueous Electrolyte for Sodium-Ion Batteries. *ACS Energy Lett.* **2017**, *2*, 2005–2006.

(20) Zhang, H.; Qin, B.; Han, J.; Passerini, S. Aqueous/Nonaqueous Hybrid Electrolyte for Sodium-Ion Batteries. *ACS Energy Lett.* **2018**, *3*, 1769–1770.

(21) Ma, L.; Schroeder, M. A.; Borodin, O.; Pollard, T. P.; Ding, M. S.; Wang, C.; Xu, K. Realizing high zinc reversibility in rechargeable batteries. *Nat. Energy* **2020**, *in press*, 10.1038/s41560–020–0674–x.

(22) Wan, F.; Zhu, J.; Huang, S.; Niu, Z. High-Voltage Electrolytes for Aqueous Energy Storage Devices. *Batteries & Supercaps* **2020**, *3*, 323–330.

(23) Suo, L.; Borodin, O.; Sun, W.; Fan, X.; Yang, C.; Wang, F.; Gao, T.; Ma, Z.; Schroeder, M.; von W. Cresce, A.; Russell, S. M.; Armand, M.; ang K. Xu, A. A.; Wang, C. Advanced High-Voltage Aqueous Lithium-Ion Battery Enabled by "Water-in-Bisalt" Electrolyte. *Angew. Chem. Int. Ed.* **2016**, *55*, 7136–7141.

(24) Forero-Saboya, J.; Hosseini-Bab-Anari, E.; Abdelhamid, M. E.; Moth-Poulsen, K.; Johansson, P. Water-in-Bisalt Electrolyte with Record Salt Concentration and Widened Electrochemical Stability Window. *J. Phys. Chem. Lett.* **2019**, *10*, 4942–4946.

(25) Chen, L. et al. A 63 m Superconcentrated Aqueous Electrolyte for High-Energy Li-Ion Batteries. *ACS Energy Lett.* **2020**, *5*, 968–974.

(26) Dubouis, N.; Park, C.; Deschamps, M.; Abdelghani-Idrissi, S.; Kanduc, M.; Colin, A.; Salanne, M.; Dzubiella, J.; Grimaud, A.; Rotenberg, B. Chasing Aqueous Biphasic Systems from Simple Salts by Exploring the LiTFSI/LiCl/H_2O Phase Diagram. *ACS Cent. Sci.* **2019**, *5*, 640–643.

(27) Yang, C.; Chen, J.; Ji, X.; Pollard, T. P.; Lü, X.; Sun, C.-J.; Hou, S.; Liu, Q.; Liu, C.; Qing, T.; Wang, Y.; Borodin, O.; Ren, Y.; Xu, K.; Wang, C. Aqueous Li-ion Battery Enabled by Halogen Conversion–Intercalation Chemistry in Graphite. *Nature* **2019**, *569*, 245–253.

(28) Lukatskaya, M. R.; Feldblyum, J. I.; Mackanic, D. G.; Lissel, F.; Michels, D. L.; Cui, Y.; Bao, Z. Concentrated mixed cation acetate "water-in-salt" solutions as green and low-cost high voltage electrolytes for aqueous batteries. *Energy Environ. Sci.* **2018**, *11*, 2876–2883.

(29) Han, J.; Mariani, A.; Zhang, H.; Zarrabeitia, M.; Gao, X.; Vieira Carvalho, D.; Varzi, A.; Passerini, S. Gelified acetate-based water-in-salt electrolyte stabilizing hexa-

cyanoferrate cathode for aqueous potassium-ion batteries. *Ener. Storage Mater.* **2020**, *30*, 196–205.

(30) Han, J.; Zarrabeitia, M.; Mariani, A.; Jusys, Z.; Hekmatfar, M.; Zhang, H.; Geiger, D.; Kaiser, U.; Behm, R. J.; Varzi, A.; Passerini, S. Halide-free water-in-salt electrolytes for stable aqueous sodium-ion batteries. *Nano Energy* **2020**, *77*, 105176.

(31) Jankowski, P.; Andersson, R.; Johansson, P. Designing High-Performant Lithium Battery Electrolytes by Utilizing Two Natures of Li+ Coordination: LiTDI/LiTFSI in Tetraglyme. *Batteries & Supercaps* **2020**, *DOI: 10.1002/batt.202000189*.

(32) Liu, X.; Elia, G. A.; Gao, X.; Qin, B.; Zhang, H.; Passerini, S. Highly Concentrated KTFSI : Glyme Electrolytes for K/Bilayered-V_2O_5 Batteries. *Batteries & Supercaps* **2020**, *3*, 261–267.

(33) Gouveia, A. S. L.; Bernardes, C. E. S.; Tomé, L. C.; Lozinskaya, E.; Vygodskii, Y.; Shaplov, A. S.; Lopes, J. N. C.; Marrucho, I. M. Ionic liquids with anions based on fluorosulfonyl derivatives: from asymmetrical substitutions to a consistent force field model. *Phys. Chem. Chem. Phys.* **2017**, *19*, 29617–29624.

(34) Ferrario, M.; Ciccotti, G.; Spohr, E.; Cartailler, T.; Turq, P. Solubility of KF in water by molecular dynamics using the Kirkwood integration method. *J. Chem. Phys.* **2002**, *117*, 4947–4953.

(35) Faber, T. E.; Ziman, J. M. A theory of the electrical properties of liquid metals. *Phil. Mag.* **1965**, *11*, 153–173.

(36) Mariani, A.; Dattani, R.; Caminiti, R.; Gontrani, L. Nanoscale Density Fluctuations in Ionic Liquid Binary Mixtures withNonamphiphilic Compounds: First Experimental Evidence. *J. Phys. Chem. B* **2016**, *120*, 10540–10546.

(37) Mariani, A.; Bonomo, M.; Passerini, S. Statistic-Driven Proton Transfer Affecting Nanoscopic Organization in an Ethylammonium Nitrate Ionic Liquid and 1,4-Diaminobutane Binary Mixture: A Steamy Pizza Model. *Symmetry* **2019**, *11*, 1425.

(38) Campetella, M.; Mariani, A.; Sadun, C.; Wu, B.; Castner Jr., E. W.; Gontrani, L. Structure and dynamics of propylammonium nitrate-acetonitrile mixtures: An intricate multi-scale system probed with experimental and theoretical techniques. *J. Chem. Phys.* **2018**, *148*, 134507.

(39) Yang, R.; Zhang, Y.; Takechi, K.; Maginn, E. J. Investigation of the Relationship between Solvation Structure and Battery Performance in Highly Concentrated Aqueous Nitroxy Radical Catholyte. *J. Phys. Chem. C* **2018**, *122*, 13815–13826.

(40) Nilsson, V.; Bernin, D.; Brandell, D.; Edström, K.; Johansson, P. Interactions and Transport in Highly Concentrated LiTFSI-based Electrolytes. *ChemPhysChem* **2020**, *21*, 1166–1176.

(41) Allen, M. P.; Tildesley, D. J. *Computer simulations of liquids*; Oxford University Press, 1987.

(42) Li, Z.; Bouchal, R.; Mendez-Morales, T.; Rollet, A.-L.; Rizzi, C.; Le Vot, S.; Favier, F.; Rotenberg, B.; Borodin, O.; Fontaine, O.; Salanne, M. Transport properties of Li-TFSI water-in-salt electrolytes. *J. Phys. Chem. B* **2019**, *123*, 10514–10521.

(43) Self, J.; Fong, K. D.; Persson, K. A. Transport in Superconcentrated $LiPF_6$ and $LiBF_4$/Propylene Carbonate Electrolytes. *ACS Energy Lett.* **2019**, *4*, 2843–2849.

(44) Xu, K. Nonaqueous Liquid Electrolytes for Lithium-Based Rechargeable Batteries. *Chem. Rev.* **2004**, *104*, 4303–4417.

(45) Lin, Z.; Goikolea, E.; Balducci, A.; Naoi, K.; Taberna, P.-L.; Salanne, M.; Yushin, G.;

Simon, P. Materials for supercapacitors: When Li-ion battery power is not enough. *Mater. Today* **2018**, *21*, 419–436.

(46) Yeh, I.-C.; Hummer, G. System-Size Dependence of Diffusion Coefficients and Viscosities from Molecular Dynamics Simulations with Periodic Boundary Conditions. *J. Phys. Chem. B* **2004**, *108*, 15873–15879.

(47) Liu, H.; Maginn, E. Effect of ion structure on conductivity in lithium-doped ionic liquid electrolytes: A molecular dynamics study. *J. Chem. Phys.* **2013**, *139*, 114508.

(48) Docampo-Álvarez, B.; Gómez-González, V.; Montes-Campos, H.; Otero-Mato, J. M.; Méndez-Morales, T.; Cabeza, O.; Gallego, L. J.; Lynden-Bell, R. M.; Ivanistsev, V. B.; Fedorov, M. V.; Varela, L. M. Molecular dynamics simulation of the behaviour of water in nano-confined ionic liquid–water mixtures. *J. Phys.: Condens. Matter* **2016**, *28*, 464001(1)–464001(8).

(49) Chen, M.; Wu, J.; Ye, T.; Ye, J.; Zhao, C.; Bi, S.; Yan, J.; Mao, B.; Feng, G. Adding Salt to Expand Voltage Window of Humid Ionic Liquids. *Nat. Commun.* **2020**, *11*, 5809.

(50) Wang, J.; Yamada, Y.; Sodeyama, K.; Chiang, C. H.; Tateyama, Y.; Yamada, A. Superconcentrated electrolytes for a high-voltage lithium-ion battery. *Nat. Commun.* **2016**, *7*, 1–9.

(51) Brehm, M.; Kirchner, B. "TRAVIS - A free Analyzer and Visualizer for Monte Carlo and Molecular Dynamics Trajectories". *J. Chem. Inf. Model.* **2011**, *51*, 2007–2023.

(52) Brehm, M.; Weber, H.; Thomas, M.; Hollóczki, O.; Kirchner, B. Domain Analysis in Nanostructured Liquids: A Post-Molecular Dynamics Study at the Example of Ionic Liquids. *Chem. Phys. Chem.* **2015**, *16*, 3271–3277.

(53) Elfgen, E.; Hollóczki, O.; Kirchner, B. A Molecular Level Understanding of Template Effects in Ionic Liquids. *Acc. Chem. Res.* **2017**, *50*, 2949–2957.

(54) Dubouis, N.; Serva, A.; Berthin, R.; Jeanmairet, G.; Porcheron, B.; Salager, E.; Salanne, M.; Grimaud, A. Tuning water reduction through controlled nanoconfinement within an organic liquid matrix. *Nat. Catal.* **2020**, *3*, 656–663.

(55) Plimpton, S. Fast Parallel Algorithms for Short-Range Molecular Dynamics. *J. Comp. Phys.* **1995**, *117*, 1–19.

(56) Martínez, L.; Andrade, R.; Birgin, E. G.; Martínez, J. M. PACKMOL: a package for building initial configurations for molecular dynamics simulations. *J. Comput. Chem.* **2009**, *30*, 2157–2164.

(57) Berendsen, H. J. C.; Grigera, J. R.; Straatsma, T. P. The Missing Term in Effective Pair Potentials. *J. Phys. Chem.* **1987.**, *91*, 6269—6271.

(58) Lopes, J. N. C.; Deschamps, J.; Pádua, A. A. H. Modeling Ionic Liquids Using a Systematic All-Atom Force Field. *J. Phys. Chem. B* **2004**, *108*, 2038–2047.

(59) Hoover, W. G. Canonical dynamics: equilibrium phase-space distributions. *Phys. Rev. A* **1985**, *31*, 1695–1697.

(60) Melchionna, S.; Ciccotti, G.; Holian, B. L. Hoover npt dynamics for systems varying in shape and size. *Mol. Phys.* **1993**, *78*, 533–544.

(61) Martyna, G. J.; Klein, M. L.; Tuckerman, M. Nosé–hoover chains: The canonical ensemble via continuous dynamics. *J. Chem. Phys.* **1992**, *97*, 2635–2643.